Ni-Cr/陶瓷连接界面残余应力有限元分析

朱　松[1]，　周振平[2]，　邱小明[3]
(1. 吉林大学 口腔医学院口腔修复科，长春　130021；2. 吉林大学 机械科学与工程学院，长春　130022；
3. 吉林大学 材料科学与工程学院，长春　130022)

摘　要：采用有限元法分析 Ni-Cr 合金与陶瓷连接冷却过程中界面残余应力形成的大小和分布特征．结果表明，Ni-Cr 合金与陶瓷存在较大的线膨胀系数差，在界面间会产生较大的残余应力，并因为边缘效应在拐角处产生应力集中，残余应力最大值出现在 Ni-Cr/陶瓷界面的近瓷侧，可达 131 MPa．Ni-Cr/陶瓷界面残余应力 σ_z 较大值出现在 Ni-Cr/陶瓷界面近瓷侧的狭小区域内，剪应力 τ_{zx} 的较大值出现在金/瓷界面，向合金和陶瓷两侧递减．采用钛中间层缓解了 Ni-Cr/陶瓷界面残余应力，使残余应力向钛中间层转移，残余应力 σ_z 较大值出现在钛中间层，剪应力 τ_{zx} 最大值出现在 Ni-Cr/Ti 界面；随着钛中间层厚度增加，界面残余应力 σ_z 增大，剪应力 τ_{zx} 变化不大．

关键词：Ni-Cr 合金；陶瓷；残余应力；有限元；钛中间层
中图分类号：TG425.2　　**文献标识码**：A　　**文章编号**：0253－360X(2012)02－0045－04

朱　松

0 序　　言

Ni-Cr 合金与陶瓷材料间存在较大的线膨胀系数差，经高温烤瓷冷却过程中导致金/瓷界面产生较大的残余应力，并永久保留在金属烤瓷修复体内的应力，对金/瓷界面结合强度影响较大[1-3]．近年来，倍受关注的界面残余应力诱发的应力集中是导致修复体制作过程中失败的主要原因越来越受到研究者重视，认为残余应力是影响界面结合强度重要因素之一[4,5]．

有限元法是伴随计算机软件、硬件技术发展起来的机构分析法，在材料连接界面残余应力的分析中已经得到应用[6]．有限元法可分析出界面处残余应力的变化趋势，也可进行量化分析结果．采用 ALGOR R13 作为软件平台，分析了 Ni-Cr 合金与陶瓷连接界面及采用金属中间层的界面残余应力形成的大小和分布特征．

1 试验方法

1.1 简化与假设

根据 Ni-Cr 合金与陶瓷连接时界面的实际情况作如下假设．

(1) Ni-Cr 合金与陶瓷连接界面是连续和完全接触，忽略界面反应，边界按理想规则形状计算．

(2) 在金属烤瓷修复体冷却过程中，温度场均匀与外界环境一致，只考虑始末两态．

(3) 金/瓷接触界面的尺寸相对于金属和陶瓷的厚度尺寸要大得多，把问题简化成平面应变问题．

(4) 假定整个烤瓷系统最初所处的高温烤瓷状态为应力自由状态．

烤瓷金属与陶瓷材料的线膨胀系数、弹性模量、泊松比和玻璃态转变温度等对 Ni-Cr/陶瓷界面残余应力的影响较大，如表 1 所示．表 2 为烤瓷工艺参数在烤瓷冷却过程中(烤瓷温度≤585 ℃)，瓷粉由熔融状态(即应力为零状态)逐渐冷却至室温，呈固态．冷却过程中因合金与陶瓷材料的线膨胀系数不同产生，并永久保留在金属烤瓷修复体内的应力，对金/瓷界面结合强度影响较大．

表 1　材料的主要性能

Table 1　Main properties of materials

	线膨胀系数 $\alpha_l/10^{-6}\mathrm{K}^{-1}$	弹性模量 E/GPa	泊松比 μ	玻璃态转变温度 $T/℃$
Ni-Cr 合金	14.3	169	0.30	—
遮色瓷	12.2	83	0.30	585
体瓷	13.3	83	0.31	585
钛	8.5	106	0.34	—

收稿日期：2011－08－23
基金项目：吉林省科技发展基金资助项目(2050511)

表 2 烤瓷工艺参数

Table 2 Firing technological parameters

烤瓷过程	起始温度 T_1/℃	预热时间 t_1/min	升温速度 v/(℃·min^{-1})	烤瓷温度 T_2/℃	烤瓷时间 t/min	真空度 p/hPa	冷却方式
遮色瓷(1)	680	1	60	990	2.5	50	空冷
遮色瓷(2)	680	1	60	990	2.5	50	空冷
体瓷	680	2	60	990	2.5	50	空冷

基于以上假设和分析，为简化模型和抓住问题的主要方面，计算转化成线弹性有限元分析.

1.2 建立模型和划分网格

采用线性有限元程序 ALGOR R13 作为有限元模拟软件环境. 根据试验实际情况，几何模型的尺寸为 Ni-Cr 合金 10 mm×15 mm×1.0 mm，遮色瓷 10 mm×10 mm×0.2 mm，体瓷 10 mm×10 mm×0.9 mm.

针对连接界面的结构特点，有限元网格的划分选用 8 节点立方体实体单元. 有限元实体模型的网格划分如图 1 所示，采用钛中间层的有限元实体模型采取网格局部细分.

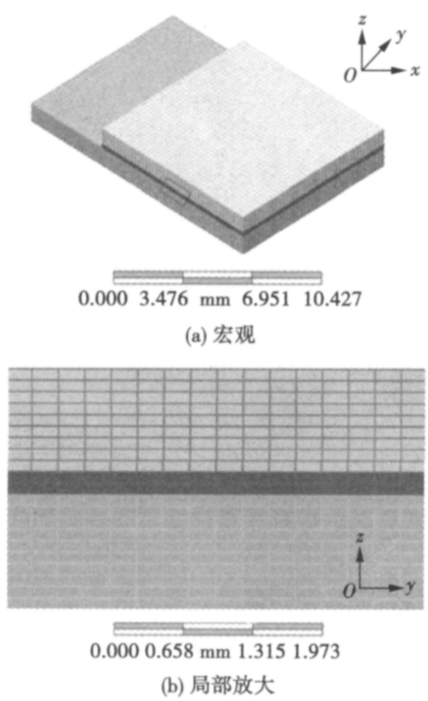

图 1 有限元分析网格划分

Fig. 1 Mesh used for residual stress by finite element analysis

2 计算结果与讨论

2.1 Ni-Cr/陶瓷连接界面残余应力分析

Ni-Cr/陶瓷界面断裂属于双材料界面断裂，由于其两侧合金和陶瓷材料性质不同，使界面断裂变得异常复杂. 在裂纹前方的界面上有正应力和剪应力，在裂纹面上既有张开位移又有滑开位移，因此 Ni-Cr/陶瓷界面断裂属于含有Ⅰ型断裂和Ⅱ型断裂的复合断裂，该复合断裂包含两种应力强度因子(K). 界面断裂力学复合应力强度因子的模式混合度指界面裂纹Ⅰ型和Ⅱ型的相互作用程度，文献[7]中建立了双材料界面裂纹扩展的有限元计算模型，得出了 K_{I} 的绝对值 > K_{II} 的绝对值. 因此，Ni-Cr/陶瓷界面裂纹断裂的过程中，张开型断裂趋向要比滑开型断裂趋向大，说明 σ_z 对界面裂纹的产生起主导地位，τ_{zx} 对界面裂纹的扩展起促进作用.

图 2 是 Ni-Cr/陶瓷连接界面残余应力分布的有限元分析结果. 由图 2 可见，金/瓷界面近 Ni-Cr 合金侧的 σ_z 为拉应力，整个界面分布均匀，沿着垂直界面方向向金属侧逐渐减小；瓷层内部受压应力，沿着垂直界面方向向瓷侧逐渐减小并逐渐转为拉应力. 剪应力 τ_{zx} 分布均匀，如图 2b 所示.

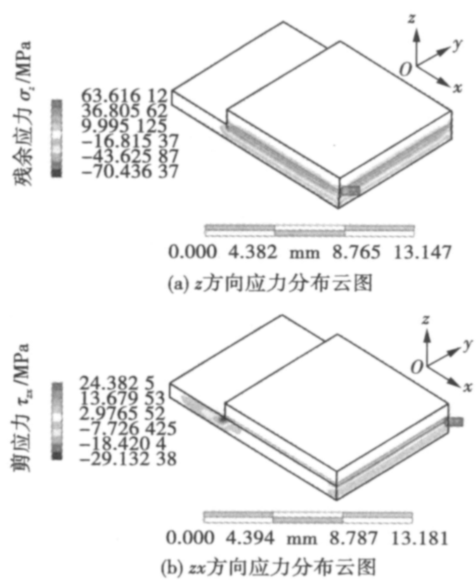

图 2 Ni-Cr/陶瓷连接界面残余应力分布

Fig. 2 Residual stress distribution in Ni-Cr/porcelain interface

由等效应力分布可知，残余应力较大区域分布

在 Ni-Cr/陶瓷界面及其附近区域，并因为边缘效应在拐角处产生应力集中，残余应力的最大值出现在 Ni-Cr/陶瓷界面的近瓷侧，可达 131 MPa. 力学性能测试时 Ni-Cr/陶瓷连接界面断裂发生在 Ni-Cr/陶瓷界面的近瓷侧. 力学性能测试时，残余应力最大值所在的 Ni-Cr/陶瓷界面的近瓷区成为薄弱环节，断裂位置多发生在此处，与模拟分析结果吻合.

图 3 是 Ni-Cr/陶瓷连接界面 $x = 14.5$ mm，$y = 5$ mm 处的残余应力沿 z 轴分布. Ni-Cr/陶瓷连接界面的金属侧受拉应力，陶瓷侧受压应力；垂直于界面的应力 σ_z 由金属底面向中心部位逐渐增大，在金属中心部分达最大值，向金/瓷连接界面位置逐渐减小，趋向于瓷侧的 σ_z 转变为压应力，临近陶瓷层表面变化平缓. Ni-Cr/陶瓷连接界面的金属侧所受的的剪应力 τ_{zx}是沿 x 轴的正方向，陶瓷侧沿 x 轴的负方向，剪应力 τ_{zx}值在 Ni-Cr/陶瓷界面达最大，向金属和陶瓷两侧递减，逐渐减小趋于零. Ni-Cr 合金中裂纹产生在夹杂和缩孔等缺陷处，裂纹向界面扩展，终止于界面处；产生在界面的裂纹沿平行界面的方向扩展，逐渐向瓷层内部偏移，且裂纹扩展边缘是锐利的[8]. 在金属烤瓷修复体冷却过程中，瓷层表层先冷却，中部后冷却，瓷表层温度低于中部，瓷表层收缩大于中部，使表层向中部施加压应力，中部向表层施加张应力，而裂纹总是选择压应力小或张应力大的区域扩展. 经分析 σ_z 和 τ_{zx}的分布特征与微观分析中裂纹的产生位置、扩展途径趋势一致.

2.2　Ni-Cr/Ti/陶瓷连接界面残余应力分析

选择钛作为中间层主要是考虑钛是活性金属中间层，可以与 Ni-Cr 合金和陶瓷同时发生相互作用，形成反应产物，并通过生成的反应产物实现 Ni-Cr 合金与陶瓷的连接. 图 4 是 Ni-Cr/Ti/陶瓷连接界面残余应力分布. 由图 4 可见，Ni-Cr/Ti 连接界面的近 Ni-Cr 合金侧的 σ_z 为拉应力，近钛侧的 σ_z 为压应力；钛中间层中的 σ_z 为大部分为拉应力；而瓷层内部 σ_z 为压应力，分布均匀. Ni-Cr/Ti/陶瓷界面残余应力 σ_z 较大值出现在钛中间层. 与 Ni-Cr/陶瓷连接界面残余应力比较，Ni-Cr/Ti/陶瓷连接界面中 Ni-Cr 合金和陶瓷中的 σ_z 分布均匀，应力值变小，变化趋势向钛中间层集中，较大的 σ_z 应力值分布区域在界面位置变宽，σ_z 最大值出现在钛/瓷界面近钛侧. 剪应力 τ_{zx}分布趋势与 Ni-Cr/陶瓷连接界面相似，应力值变小.

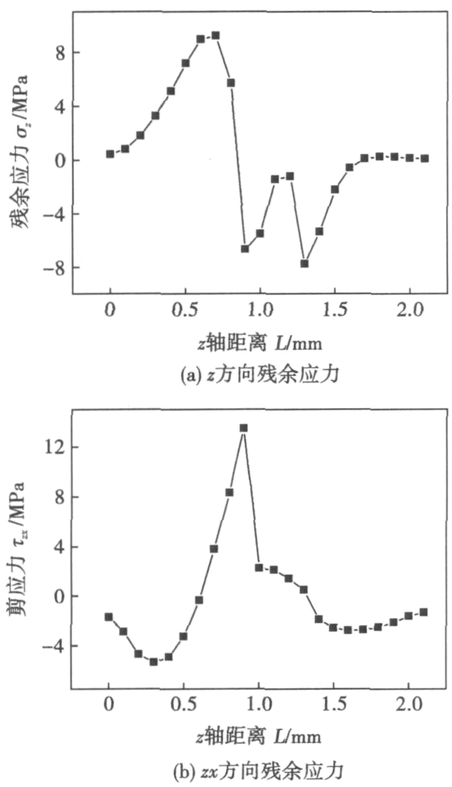

图 3　Ni-Cr/陶瓷连接界面 $x = 14.5$ mm，$y = 5$ mm 处的残余应力

Fig. 3　Residual stress distribution in Ni-Cr/porcelain interface at $x = 14.5$ mm，$y = 5$ mm

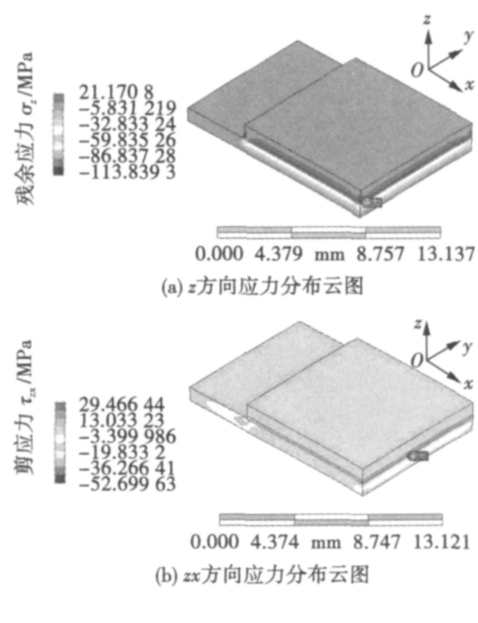

图 4　Ni-Cr/Ti/陶瓷连接界面残余应力分布

Fig. 4　Residual stress distribution in Ni-Cr/Ti/porcelain interface

由等效应力图分析可知 Ni-Cr/Ti/陶瓷连接界面残余应力分布均匀，残余应力较大区域分布在钛中间层及其附近区域，残余应力最大值出现在钛/瓷界面近钛侧，可达 207 MPa. 结果表明，钛中间层将 Ni-Cr/Ti/陶瓷连接界面处的残余应力转移到中间

层上,致使 Ni-Cr 合金和陶瓷中应力分布均匀,使 Ni-Cr 合金和陶瓷两者内部的裂纹缺陷发生几率减少.

图5是 Ni-Cr/Ti/陶瓷连接界面 x = 14.5 mm,y = 5 mm 处的残余应力沿 z 轴分布. 由图5可见,采用钛中间层时,Ni-Cr 合金侧区域 σ_z 为正值拉应力,σ_z 由 Ni-Cr 合金底面向中心部位逐渐增大,在 Ni-Cr 合金中心部分达最大值,然后向 Ni-Cr/Ti 界面逐渐减小,趋向于界面边界点逐渐转为负值压应力,而在钛中间层 σ_z 又由负值转变为正直,钛中间层大部分受拉应力,临近钛/瓷界面变化逐渐转变为负值,瓷层部分全受压应力. 剪应力 τ_{zx} 在 Ni-Cr/Ti 界面为正值达最大,向 Ni-Cr 合金和陶瓷两侧递减,逐渐减小为负值,最后趋向为零. 与 Ni-Cr/Ti/陶瓷连接界面时相比,采用钛中间层改善了 Ni-Cr/Ti/陶瓷界面的残余应力 σ_z 的大小和分布位置,缓解了 Ni-Cr 合金和陶瓷内部的应力,使残余应力向钛中间层转移;同时钛中间层改善了界面残余应力的大小. 随着钛中间层厚度的增加,界面残余应力增大,剪应力 τ_{zx} 变化不大. 进一步说明,钛中间层厚度越大,残余应力 σ_z 越大,界面产生裂纹缺陷几率越大,这将直接

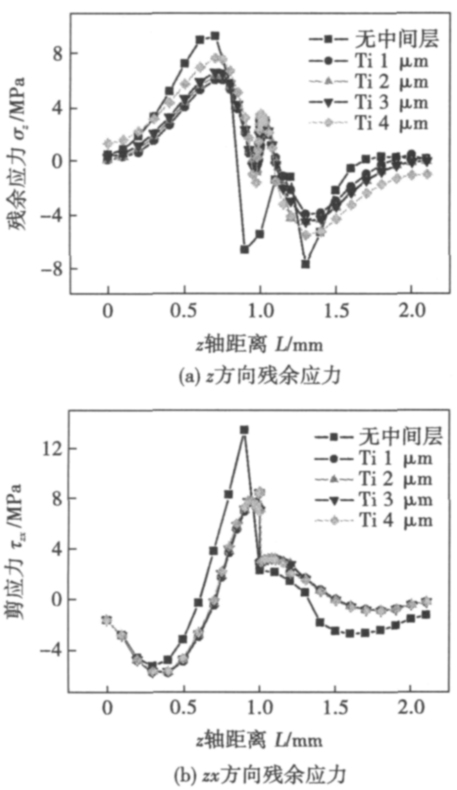

图5 Ni-Cr/Ti/陶瓷连接界面 x = 14.5 mm, y = 5 mm 处的残余应力沿 z 轴分布

Fig. 5 Residual stress distribution in Ni-Cr/Ti/porcelain interface along z direction at x = 14.5 mm, y = 5 mm

影响界面结合强度. 当钛中间层厚度太小时,熔融的瓷粉不能与钛中间层充分润湿、反应,起不到很好的连接作用,导致界面结合强度降低. 因此,钛中间层厚度的选取是一个多因素综合考虑的过程. 钛中间层是将修复体内的残余应力转移到中间层中,致使 Ni-Cr 合金和陶瓷内部的残余应力分布均匀、应力值变小,较大的残余应力分布在钛中间层区域内,这将减少 Ni-Cr 合金和瓷层内部裂纹发生.

3 结 论

(1) Ni-Cr/陶瓷连接界面残余应力 σ_z 较大值出现在 Ni-Cr/陶瓷界面近瓷侧的狭小区域内,可达 131 MPa; 剪应力 τ_{zx} 的较大值出现在金/瓷界面,向合金和陶瓷两侧递减. 残余应力的最大值出现在 Ni-Cr/陶瓷界面的近瓷层.

(2) Ni-Cr/Ti/陶瓷连接界面残余应力较大值出现在钛中间层; 剪应力的最大值出现在 Ni-Cr/Ti 界面. 与 Ni-Cr/陶瓷连接界面残余应力比较,采用钛中间层缓解了 Ni-Cr 合金和陶瓷内部的应力,使残余应力向钛中间层转移; 随着钛中间层厚度的增加,界面残余应力 σ_z 增大. 在保证界面充分反应的同时,应尽量选择较小的中间层厚度.

参考文献:

[1] 辛海涛, 马轩祥, 李玉龙, 等. 金-瓷修复体粘弹性残余应力的有限元分析[J]. 华西口腔医学, 2004, 22(6): 463-473.
Xin Haitao, Ma Xuanxiang, Li Yulong, *et al*. The study of viscoelastic residual stresses of ceramic-metal bond [J]. West China Journal of Stomatology, 2004, 22(6): 463-473.

[2] Xin Haitao, Li Yulong, Ma Xuanxiang, *et al*. The investigation of residual stress effect on metal-ceramic bond [J]. Key Engineering Materials, 2004, 274-276(1): 1065-1070.

[3] Anusavice K J, Dehoff P H. Comparative evaluation of ceramic-metal bond tests using finite element stress analysis [J]. Materials Science, 1980, 59(3): 608-613.

[4] Tesk J A, Asaoka K. Transient and residual stress in a porcelain-metal strip [J]. Journal of Dental Reserach, 1990, 69: 463-469.

[5] Wang Dongmei, Zhang Xiuyin. Study on interfacial fracture behaviors of the porcelain-fused-to-metal restoration by moiré interferometry method and finite element analysis [J]. The International Society for Optical Engineering, 2001, 4537: 233-236.

[6] Sato Takuya, Kobayashi, Hideo, *et al*. Finite-element analysis of residual stresses of ceramic/metal joints [J]. Transactions of the Japan Society of Mechanical Engineers, 1991, 57(543): 2702-2707.

[下转第52页]

性能;但是如果碳纳米管含量过高,其在界面上的分布越多,与铝反应生成的碳化铝就越多,最终会有损于碳纳米管与铝基体之间的界面结合,破坏熔核性能. 随着碳纳米管含量的增加,碳化铝的生成量逐渐增加,界面结合遭到破坏,晶界逐渐变粗.

4 结 论

(1) 在铝合金熔核中添加碳纳米管能显著提高熔核的硬度和强度,且熔核的晶粒尺寸明显减小,在扫描电镜下能够看到碳纳米管均匀分布在熔核中,且与基体的界面结合良好.

(2) 碳纳米管在熔核中的强化机制主要是载荷传递、位错增殖、约束变形以及细晶强化.

参考文献:

[1] 肖亚庆. 中国铝工业技术发展[M]. 北京: 冶金工业出版社, 2007.

[2] 李 杰, 宋仁国, 陈小明, 等. 7050 高强铝合金强化固溶处理研究[J]. 热加工工艺, 2009(6): 125 - 128.
Li Jie, Song Renguo, Chen Xiaoming, *et al*. Study on strengthening solution treatment for 7050 high strength aluminum alloy[J]. Hot Working Technology, 2009(6): 125 - 128.

[3] 李青松. 铝合金点焊熔核设计[D]. 天津: 天津大学, 2007.

[4] 吴 林, 陈善本. 智能化焊接技术[M]. 北京: 国防工业出版社, 2000.

[5] Iijima S. Helical microtubes of graphitic carbon[J]. Nature, 1991, 354(6): 56 - 58.

[6] Treacy M M J, Ebbesen T W, Gibson J M. Exceptionally high Young's modulus observed for individual carbon nanotubes[J]. Nature, 1996, 381(5): 678 - 682.

[7] Barrera E V, Sims J, Callahan D L. Processing of fullerene-reinforced composites[J]. J Mate Res, 1994, 10(9): 2662 - 2669.

作者简介: 王 皓,男,1987 年出生,硕士研究生. 主要从事电阻点焊工艺、激光焊接质量检测以及焊接材料方面的研究. 发表论文 1 篇. Email: mars-wanghao@qq.com

通讯作者: 罗 震,男,教授,博士生导师. Email: Lz@tju.edu.cn

[上接第 48 页]

[7] Mi Honglin, Fang Ruhua. Finite element analysis of material interfacial fracture intensity in porcelain-fused-to-metal restoration [J]. Journal of Tongji University, 2005, 33(1): 98 - 103.

[8] 刘 杰, 邱小明, 孙大谦, 等. Ni-Cr 合金烤瓷材料界面组织结构和力学性能的研究[J]. 吉林大学学报工学版, 2007, 37(5): 1083 - 1087.
Liu Jie, Qiu Xiaoming, Sun Daqian, *et al*. Study on the interface microstructure and mechanical properties of Ni-Cr alloy porcelain materials[J]. Journal of Jilin University (Engineering Edition), 2007, 37(5): 1083 - 1087.

作者简介: 朱 松,男,1965 年出生,博士,教授. 主要从事新材料连接和口腔临床工作. 发表论文 20 余篇. Email: zhusong1965@163.com

通讯作者: 邱小明,男,教授,博士研究生导师. Email: qiuxm@jlu.edu.cn

methods applied in seam tracking.

Key words: image processing; seam tracking; centerline; linearity; the least-square method

Microstructure and properties of Fe-W composite coating by laser cladding WU Yang, YU Gang, HE Xiuli, NING Weijian (Key Laboratory of Mechanics in Advanced Manufacturing, Institute of Mechanics, Chinese Academy of Sciences, Beijing 100190, China). pp 37 –40, 44

Abstract: An investigation of laser cladding Fe-W composite coating on Q235 steel was performed by injection of tungsten powder. The microstructure of the coating was analyzed with X-ray diffraction (XRD), optical microscope, scanning electron microscopy (SEM) and energy disperse spectroscopy (EDS). The microhardness and wear resistance were examined by hardness tester and abrading machine. The coating was metallurgically bonded with the substrate without visible crack or pore. The clad layer had a microstructure consisting of primary coarse dendrite or short stick Fe_7W_6 and fine isolated Fe_2W particles which uniformly dispersed in the α-Fe matrix. The average microhardness of the clad layer was approximately 700 HV which was 3.5 times greater than that of the Q235 substrate. The wear resistance was also obviously improved.

Key words: laser cladding; coaxial powder injection; Fe-W composite coating; microhardness; wear resistance

Numerical study on influence of axial pressure on inertia friction welding WANG Feifan, LI Wenya, CHEN Liang, LI Jinglong (State Key Laboratory of Solidfication Processing, Shanxi Key Laboratory of Friction Welding Technologies, Northwestern Polytechnical University, Xi'an 710072, China). pp 41 –44

Abstract: A 2-D finite element model of inertia friction welding of GH4169 tubular was established based on the ABAQUS environment. The effect of axial pressure on the temperature field and axial upset of the joint was investigated by adopting the remeshing technique. The variations of joint temperature field under different axial pressures were also expounded. Moreover, according to the change of axial upset, the effect of axial pressure on the flash shape was analyzed. The results show that increasing axial pressure can significantly raise the conversion efficiency from flywheel kinetic energy to weld heat, shorten the time to high temperature quasi-steady state, and obtain flash shape. However, an extensively large pressure is negative to temperature field uniformity, which may result in bad stress concentration. At last, the pressure of 400 MPa is supposed to be a good parameter in this study.

Key words: inertia friction welding; axial pressure; temperature field; flash shape

Finite element modeling of residual stress in bonding interface of Ni-Cr/porcelain ZHU Song[1], ZHOU Zhenping[2], QIU Xiaoming[3] (1. College of Stomatology, Jilin University, Changchun 130021, China; 2. College of Machanical Science and Engineering, Jilin University, Changchun 130022, China; 3. College of Materials Science and Engineering, Jilin University, Changchun 130022, China). pp 45 –48, 52

Abstract: The numerical value and distribution of residual stress in the bonding interface of Ni-Cr/porcelain and Ni-Cr/Ti/porcelain have been investigated by finite element method. The experimental results show that there is much difference in thermal expansion coefficient between Ni-Cr alloy and proclaim. Larger residual stress will be produced at the interface. Due to produced stress concentration at the corner resulted in edge effect, the maximal value of residual stress is 131 MPa, which appears at the Ni-Cr alloy/proclaim interface near proclaim side. The greater σ_z value appears in a narrow area on the near porcelain side. The greater shearing stress τ_{zx} value appears in the Ni-Cr/porcelain interface, and gradually decreases to Ni-Cr alloy and porcelain sides. Residual stress and distribution position of Ni-Cr/Ti/porcelain has been improved when using Ti interlayer comparing with the residual stress of Ni-Cr/porcelain interface. Inner stress between Ni-Cr alloy and porcelain has been released and the residual stress is transferred to Ti interlayer; The thickness of Ti interlayer has effects on residual stress, the σ_z of interface is increasing and shearing stress τ_{zx} is little different with the interlayer thickness increasing.

Key words: Ni-Cr alloy; porcelain; residual stress; finite element; Ti interlayer

Study on influence of CNT to nugget of aluminum alloy spot welding WANG Hao[1,2], LUO Zhen[1,2], ZHOU Linshu[1], ZHANG Di[1,2] (1. School of Materials Science and Engineering, Tianjin University, Tianjin 300072, China; 2. Tianjin Key Laboratory of Advanced Joining Technology, Tianjin University, Tianjin 300072, China). pp 49 –52

Abstract: The process of aluminium alloy spot welding is widely used nowadays and the industry puts forward higher request in its properties and quality. The microstructure of aluminium alloy spot welding nuggets decides its macroscopic properties. In this paper, the microstructure of nugget was changed to enhance its properties and quality. Carbon nano-tube (CNT) was chosen as the addition of the aluminium alloy spot welding, and further analysis of the mechanical properties, microstructure and components of the welding spot of aluminium alloy. The results indicated that when the CNT was added in the aluminium alloy, the sizes of spot welding grain decreased significantly. The CNT distributed uniformly in the nuggets and it could increase the hardness and intensity significantly. The further analysis indicated that the carbon nano-tubes strengthening mechanism was mainly dislocation multiplication, transformation of load, constrained deformation and fine grain strengthening.

Key words: aluminum alloy; resistance spot welding; carbon nano-tube; model of strengthen theory

Microstructures and wear resistance of Ni-based PLA surfacing layer with introducing magnetic field LIU Zhengjun[1], LI Lecheng[1], ZONG Lin[1,2], SU Yunhai[1], SU Ming[1] (1. School of Material Science and Engineering, Shenyang University of Technology, Shenyang 110870, China; 2. School of Mechanical Engineering, Shenyang University of Chemical Technology, Shenyang 110142, China). pp 53 –56

Abstract: Ni-based alloy was surfaced on low-carbon steel by plasma arc surfacing under DC transverse magnetic field. The hardness, wear resistance, microstructure and phase constitution of the surfacing layers were investigated via hardness and wear tests as well as SEM, EDS and XRD analysis. The influence of DC transverse magnetic field on the microstructures and wear resistance of the surfacing layer, the shape and amount of the hard phase were systematically studied. Furthermore, pre-